

Macromolecular Import into *Escherichia coli*: The TolA C-Terminal Domain Changes Conformation When Interacting with the Colicin A Toxin[†]

Christophe Deprez,[‡] Laurence Blanchard,^{*,‡} Françoise Guerlesquin,[§] Marthe Gavioli,^{||} Jean-Pierre Simorre,[‡] Claude Lazdunski,^{||} Dominique Marion,[‡] and Roland Lloubès^{||}

Institut de Biologie Structurale "Jean-Pierre Ebel", CEA-CNRS-UJF, UMR 5075, 41 rue Jules Horowitz, 38027 Grenoble cedex 1, France, and Institut de Biologie Structurale et Microbiologie, CNRS, UPR 9036 and UPR 9027, 31 chemin Joseph Aiguier, 13402 Marseille cedex 20, France

Received August 27, 2001; Revised Manuscript Received December 19, 2001

ABSTRACT: Various macromolecules such as bacteriotoxins and phage DNA parasitize some envelope proteins of *Escherichia coli* to infect the bacteria. A two-step import mechanism involves the primary interaction with an outer membrane receptor or with a pilus followed by the translocation across the outer membrane. However, this second step is poorly understood. It was shown that the TolA, TolQ, and TolR proteins play a critical role in the translocation of group A colicins and filamentous bacteriophage minor coat proteins (g3p). Translocation of these proteins requires the interaction of their N-terminal domain with the C-terminal domain of TolA (TolAIII). In this work, short soluble TolAIII domains were overproduced in the cytoplasm and in the periplasm of *E. coli*. In TolAIII, the two cysteine residues were found to be reduced in the cytoplasmic form and oxidized in the periplasmic form. The interaction of TolAIII with the N-terminal domain of colicin A (A_{Th}) is observed in the presence and in the absence of the disulfide bridge. The complex formation of TolAIII and A_{Th} was found to be independent of the ionic strength. An NMR study of TolAIII, both free and bound, shows a significant structural change when interacting with A_{Th}, in the presence or absence of the disulfide bridge. In contrast, such a structural modification was not observed when TolAIII interacts with g3p N1. These results suggest that bacteriotoxins and Ff bacteriophages parasitize *E. coli* using different interactions between TolA and the translocation domain of the colicin and g3p protein, respectively.

The Tol–Pal system of *Escherichia coli* is composed of two membrane-bound protein complexes located in the cell envelope. One is located in the cytoplasmic membrane and involves the TolA, TolQ, and TolR proteins (1–3), and the other is associated with the outer membrane (4, 5) and is composed of the outer membrane-anchored Pal lipoprotein and the periplasmic TolB protein. The interaction of TolA with Pal, forming a link between the inner and outer membranes, was demonstrated to be coupled to the proton motive force of the inner membrane (6). Moreover, Pal belongs to the peptidoglycan interacting lipoproteins (7), and TolB was found to interact *in vivo* with Lpp and OmpA in a Pal-dependent behavior (8). Thus, the Tol–Pal system is tightly associated with structural components of the cell envelope. The loss of outer membrane integrity was observed for each of the *tol–pal* mutants which are leaky for periplasmic proteins, are hypersensitive to drugs and detergents (9), and release outer membrane vesicles (10), indicating that these proteins play an important role in membrane integrity (11). *In vitro*, TolA and TolB have been shown to

interact with porins (12, 13), and *in vivo*, the export of O antigen to the cell surface was found to depend on the TolA protein (14). These results indicate that the Tol–Pal system would drive newly synthesized outer membrane components across the periplasm. On the other hand, the Tol–Pal system has been parasitized and is required for the import of macromolecules such as colicins (colicins A, E1–E9, K, L, and N) and phage DNA (M13, fd, and f1) through the cell envelope (9, 15).

Colicins are plasmid-encoded bacterial toxins produced by enterobacteria. These toxins exhibit various types of lethal activity. The mechanism of cytotoxicity results from nuclease activity, the formation of ion channels in the cytoplasmic membrane, or the inhibition of peptidoglycan synthesis. Prior to their action, the import of colicins is mediated by their binding to specific receptors of the outer membrane, and their translocation through the cell envelope which requires either the Tol–Pal system (group A colicins) or the TonB system (group B colicins) (15). The three-dimensional structure of several of these toxins shows a similar type of organization (16–19). It comprises three distinct domains: the N-terminal domain involved in the translocation across the outer membrane, the central domain or receptor binding domain, and the C-terminal domain that is responsible for lethal activity. Membrane fractionation shows that the Tol proteins form a complex with imported colicin A (20) and that, during pore formation, colicin A retains interactions with its receptor

[†] This work was supported by a grant from PCV (Physique et Chimie du Vivant), the CNRS, the CEA (France), and Molecular Simulations Inc. C.D. is a recipient of a MENRT fellowship.

* To whom correspondence should be addressed. Phone: (33) 438 784 756. Fax: (33) 438 785 494. E-mail: laurence.blanchard@ibs.fr.

[‡] CEA-CNRS-UJF, UMR 5075.

[§] CNRS, UPR 9036.

^{||} CNRS, UPR 9027.

and the Tol machinery (21). A mechanism of translocation of the N-terminal domain through the OmpF channel has been proposed (18), while the process involved in the translocation of the C-terminal domain of the toxin across the outer membrane remains unknown.

Infection of *E. coli* by filamentous bacteriophages is mediated by g3p,¹ a minor coat protein located at the end of the phage capsid. The g3p protein has a modular structure composed of three domains (N1, N2, and CT) separated by glycine-rich linkers and in addition a short C-terminal transmembrane segment. The three-dimensional structure of the two N-terminal domains of g3p from phage M13 and fd has been determined (22, 23). According to the current model, infection of the host cells is initiated by binding of the g3p central domain to the tip of an F-pilus which is presumably then retracted, thereby guiding the bound phage to the cell envelope. At this stage, the interaction of the g3p N-terminal domain with the TolA protein would trigger an as yet unknown process leading to the entry of the phage DNA into the bacterial cytoplasm (24, 25).

The process of infection of *E. coli* by group A colicins and filamentous bacteriophages exhibits several analogies, including their interactions with TolA. The TolA protein consists of three domains: the N-terminal domain anchoring the protein in the cytoplasmic membrane, the central domain which is assumed to be an α -helical structure long enough to span the periplasmic space (26, 27), and the C-terminal domain (TolAIII) involved in the interaction with group A colicins and with the minor coat g3p (24, 28). The interaction between TolAIII and g3p N1 has already been characterized by NMR and X-ray crystallography (24, 29).

The aim of our work was to study the interaction between TolAIII and the N-terminal domain of colicin A and to investigate the molecular mechanism of macromolecular import into *E. coli*. Formation of the TolAIII–A_{Th} complex was studied by biochemical and biophysical methods, and compared to that of the TolAIII–g3p N1 complex.

EXPERIMENTAL PROCEDURES

Plasmid Constructions

pTolAIII. pTolAIII1 [originally called pARTolAIII (30)], pTolAIII2, and pTolAIII3 plasmids encoded the 132, 93, and 97 C-terminal residues of TolA, respectively. The proteins were tagged with six histidine residues located at their N-terminal (TolAIII1 and TolAIII2) or C-terminal (TolAIII3) extremity. pTolAIII2 was constructed following the plasmid mutagenesis protocol (31) in which one primer was designed to delete the first 39 residues of the TolAIII1 sequence. The pTolAIII1 plasmid was used as a template with two primers: 5'-aacaatggcgcacatcaggggccgatcaataactatgccg and 5'-gccctgatgcgcattgttcacgcggtgatgatgatgat. The recombinant PCR product was transformed in the DH5 α cells, and the *tolAIII2* gene was checked by DNA sequencing. The pTolAIII3 plasmid was amplified using the pTolAIII1

plasmid as a template and 5'-tatgaattcggtaataactaaaaacaatggcgc and 5'-ttaggatccttagtgatgatggtggtgatgcggttggaagtccaatggcgcg primers (the *EcoRI* and *BamHI* restriction sites are underlined). The purified PCR DNA fragment digested with *BamHI* and *EcoRI* was inserted into the pIN-III-OmpA2 vector (32), opened with the same restriction sites. pTolAIII derivative expression was regulated by the AraC (TolAIII1 and TolAIII2) or LacI (TolAIII3) repressor.

pA_{Th}. The coding sequence of the translocation domain of colicin A was amplified using pColA9 (33) as a template and 5'-ttcgtacatatgcctggattaattatggta and 5'-ttcgtctagagttagtgatgatgatgatgatgacgggaacttcacagtc primers (the *NdeI* and *XbaI* restriction sites are underlined). The PCR product was ligated in the TA cloning pTAG plasmid (R&D Systems). The *NdeI*–*HindIII* DNA fragment was purified and inserted into the pT7.7 plasmid (34) opened with the same restriction sites. The resulting plasmid pA_{Th} encoded the first 172 residues of colicin A followed by six histidine residues (A_{Th}). The *a_{Th}* gene was transcribed from the T7 promoter, and its coding sequence was checked by DNA sequencing.

pP31. This plasmid encoding the g3p N1 precursor under the control of the T7 promoter was constructed by PCR amplification using M13 replicative form DNA as a template and the primers 5'-catatgaaaaattattatcgcaattcct and 5'-ttattagtgatgatgatgatgatgcccaccaccctcat (*NdeI* restriction site underlined). The amplified DNA fragment was ligated in the pPCR-Script Cam cloning vector (Stratagene). The *NdeI*–*HindIII* DNA fragment of positive clones was purified and ligated into the pT7.7 vector digested with the same restriction enzymes. The pP31 plasmid encoded the signal sequence and the 71 N-terminal residues of g3p N1 followed by six histidine residues at the C-terminus.

Expression and Purification

A_{Th}. BL21(DE3) cells freshly transformed by pA_{Th} were grown at 30 °C. At the exponential growth phase ($A_{600} = 0.5$), the production of the protein was achieved by inducing the synthesis of chromosomal T7 RNA polymerase with 0.1 mM IPTG and incubating the cells for 16 h at 22 °C with vigorous shaking. The soluble cell extract was recovered after cell sonication and ultracentrifugation. A_{Th} was purified using the IMAC protocol, and the eluted material was further concentrated using ion exchange chromatography (MonoS, Pharmacia).

TolAIII. TolAIII2 was purified from the cytoplasm of W3110 cells following the procedure described for A_{Th} except that L-arabinose was added at a concentration of 0.5 mg/mL. TolAIII3 with the N-terminal signal sequence of OmpA was purified from the periplasm or the supernatant of W3110 cells. Cells were induced with 0.1 mM IPTG at 22 °C for 16 h. Cells were pelleted, and processed TolAIII3 was recovered from the culture supernatant and the periplasm by osmotic shock. The periplasmic protein was purified using metal affinity chromatography (IMAC) (Talon, Clontech). Extracellular proteins were purified by adding cobalt beads to the culture supernatant (at a pH adjusted to 8.0) and incubating it for 1 h with shaking. Beads were poured onto a column, and the protein was eluted with imidazole.

g3p N1. The g3p N1 domain was purified from the periplasm and the culture supernatant of BL21(DE3) cells harboring the pP31 plasmid under growth conditions similar

¹ Abbreviations: CD, circular dichroism; NMR, nuclear magnetic resonance; nOe, nuclear Overhauser effect; CSI, chemical shift index; DSS, 3-(trimethylsilyl)-1-propanesulfonic acid; TolAIII, C-terminal domain of TolA; g3p, gene 3 minor coat protein of Ff bacteriophages; A_{Th}, polyhistidine-tagged colicin A translocation domain; AT1, colicin A translocation domain.

to those used for ATh and purified following the TolAIII3 procedure.

For $^{15}\text{N}/^{13}\text{C}$ isotopic labeling experiments, W3110 or BL21(DE3) cells harboring the plasmids described above were grown in M9 minimal media using $^{15}\text{NH}_4\text{Cl}$ (1 g/L) and $[^{13}\text{C}_6]\text{glucose}$ (2 g/L) as the sole nitrogen and carbon source, respectively. Proteins were further purified as described previously. Large amounts of ATh and TolAIII derivatives were purified from the cytoplasm or the periplasm of *E. coli* (between 20 and 30 mg of ATh and TolAIII derivatives were obtained from 1 L of culture in LB or M9 medium). However, for unknown reasons, the purification of g3p gave much lower yields ($\sim 2\text{--}3$ mg/L).

Purified proteins were checked using MALDI-TOF spectrometry to verify the mass, N-terminal sequencing, and amino acid compositions. The extinction coefficients at 280 nm of ATh, TolAIII3, and TolAIII2 were calculated (29 323, 6384, and 6239 $\text{M}^{-1} \text{cm}^{-1}$ respectively). The concentration of the g3p N1 domain was calculated using a theoretical extinction coefficient of 20 910 $\text{M}^{-1} \text{cm}^{-1}$.

Biochemical Binding Assays

Overlay and SDS-PAGE shift assays were performed as previously described (28, 30). For coprecipitation experiments, ~ 4 μg of purified TolA derivatives (TolAIII2 or TolAIII3) was immobilized on cobalt beads (Talon, Clontech) and further incubated for 60 min with 6 μg of purified AT1 in 20 mM Tris-HCl (pH 8.0) in the presence of 0, 50, or 500 mM NaCl. Beads were washed with the same buffer, and immobilized material was eluted with 30 μL of 500 mM imidazole. Samples were heat denatured with loading buffer (without reducing agent) for 10 min at 96 $^\circ\text{C}$ before SDS-PAGE analyses. The co-immunoprecipitation assays were performed using 2 μM ATh and TolAIII2 or TolAIII3 proteins incubated in 50 mM potassium phosphate buffer (pH 6.8) and 50 mM NaCl. The IgG of the 1C11 monoclonal antibody (epitope located within the N-terminal domain of ATh) immobilized on protein A-Sepharose beads (Pharmacia) was added to the ATh/TolAIII mixture and further incubated for 45 min. After two washes, the proteins were eluted by adding loading buffer. The samples were heat denatured and analyzed by SDS-PAGE with Coomassie blue staining. Gel filtration experiments were performed with a Superose 12 column (Pharmacia).

NMR Spectroscopy

All NMR spectra were acquired at 300 K on 400, 600, and 800 MHz Varian Inova spectrometers equipped with triple-resonance (^1H , ^{13}C , and ^{15}N) probes, including shielded z -gradients. Parameters for all experiments can be obtained from the authors. Spectra were processed and analyzed with Felix 97 (Molecular Simulations Inc., San Diego, CA). The FIDs were typically treated with a 90 $^\circ$ -shifted sine-bell squared apodizing function, and the residual water suppression was achieved using a sine-bell convolution. Proton chemical shifts were reported with respect to the H_2O signal relative to DSS. The ^{15}N and ^{13}C chemical shifts were referenced indirectly using the $^1\text{H}/X$ frequency ratios of the zero point: 0.101 329 118 (^{15}N) and 0.251 449 530 (^{13}C) (35).

NMR Titration. ^{15}N -labeled TolAIII3 was prepared in 50 mM potassium phosphate buffer (pH 6.8), 50 mM NaCl,

protease inhibitor cocktail (Complete by Boehringer Mannheim), and 10% $^2\text{H}_2\text{O}$. The final concentration was 0.1 mM. Small aliquots of unlabeled ATh (2 mM) prepared in the same buffer (without $^2\text{H}_2\text{O}$) were added successively to the ^{15}N -labeled TolAIII3 sample to achieve the following concentrations: 0.03, 0.05, 0.08, 0.1, and 0.2 mM. After each addition, two-dimensional (2D) ^1H - ^{15}N HSQC experiments were carried out on a Varian Inova 800 MHz spectrometer. Spectral resolutions were 9.8 Hz in t_1 (^{15}N) and 11.7 Hz in t_2 (^1H). Each HSQC experiment lasted 56 min, and the spectra were recorded twice to monitor the sample stability with time. No significant difference could be detected within each pair of spectra. Free induction decays were added before further processing.

NMR Binding Assays. Typically, a concentrated unlabeled sample was added to a ^{15}N -labeled sample in 10% $^2\text{H}_2\text{O}$ to reach a 1/1 stoichiometry. Complete (Boehringer Mannheim) was used as protease inhibitor cocktail when mentioned. Before and after the addition, a 2D ^1H - ^{15}N HSQC spectrum was recorded on a Varian Inova 800 MHz spectrometer.

Steady-State Heteronuclear $n\text{Oe}$. The heteronuclear $n\text{Oe}$ value for each resonance peak of ^{15}N -labeled TolAIII3 is the ratio of the intensity in an H-saturated HSQC experiment ($\langle I_z^{SS} \rangle$) by the intensity in a standard (nonsaturated) HSQC experiment ($\langle I_z^0 \rangle$), collected on a Varian 800 MHz spectrometer. Errors were estimated from the noise levels.

Diffusion. DOSY experiments were performed at 400 MHz using a Varian Inova instrument equipped with a 5 mm triple-resonance probe with a z -axis shielded magnetic field gradient. A PFG longitudinal eddy-current delay (LED) pulse sequence was used, and a ^{13}C filter was included at the beginning of the sequence to detect the signal of the ^{13}C -labeled TolAIII3 protein only. The spectra were recorded with a recovery time of 3.5 s, 96 transients, and a diffusion time of 150 ms. Diffusion coefficients were measured by incrementing the magnitude of the field gradient pulse from 0.6 to 57 G cm^{-1} . Data were processed with the software developed by G. Morris and distributed by Varian Inc.

Mass Spectrometry

To characterize the oxidation state of disulfides, samples were digested with 1% (w/w) LysC endoprotease (2 h at 37 $^\circ\text{C}$) in 25 mM ammonium carbonate buffer (pH 7.2), and fragments were analyzed by MALDI-TOF mass spectrometry.

Circular Dichroism

Far-UV CD spectra were recorded with a 1 mm path length cell on a Jobin-Yvon UV CD spectrophotometer (CD6) at 25 $^\circ\text{C}$. For each spectrum, three scans were accumulated at 0.5 nm intervals with an integration time of 1 s. The samples were in 50 mM NaCl and 50 mM NaPO_4 (pH 6.8). Protein concentrations were 4 μM (ATh), 7 μM (TolAIII3), and 9 μM (ATh/TolAIII3 equimolar mixture).

RESULTS

Construction, Production, and Structural Characterization of TolAIII. A 2D ^1H - ^{15}N heteronuclear single-quantum correlation (HSQC) spectrum was recorded on a ^{15}N -labeled sample of the purified TolAIII1 protein (containing the 132 C-terminal residues of TolA). It proved to be unsuited for

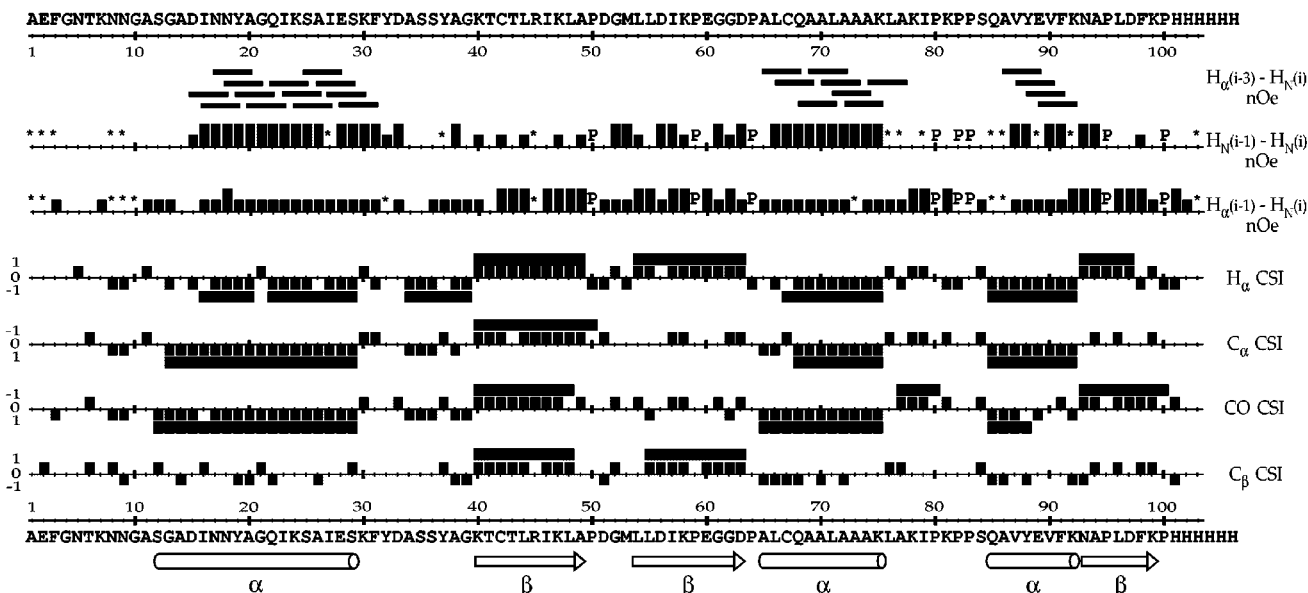


FIGURE 3: Characterization of secondary structure elements of TolAIII3. From top to bottom, $H_{\alpha(i-3)}-H_{N(i)}$ nOe correlations, sequential $H_{\alpha(i-1)}-H_{N(i)}$, and $H_{N(i-1)}-H_{N(i)}$ nOe correlations reflecting the intensity of the corresponding cross-peak in a 3D NOESY-HSQC spectrum (proline residues are denoted with the letter P; missing assignments or peak overlaps are denoted with a star). Chemical shift index (CSI) for H_{α} , C_{α} , CO, and C_{β} . Secondary structure elements (α -helices, cylinders; β -strands, arrows).

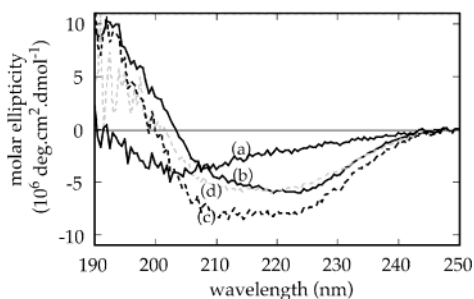


FIGURE 4: Far-UV circular dichroism of TolAIII3, Ath, and TolAIII3-Ath. (a) Molar ellipticity of Ath (—). (b) Molar ellipticity of TolAIII3 (—). (c) Theoretical molar ellipticity of an equimolar noninteracting mixture of TolAIII3 and Ath (dashed gray line), calculated from traces a and b. (d) Molar ellipticity of an equimolar TolAIII3/Ath mixture (dashed black line).

pAT1 plasmid (40). However, because TolB interacts with AT1 (41) and could therefore be a potential contaminant, new purification strategies were used. Preliminary experiments for purifying AT1 using *tolB* strains exhibited low production yields; thus, we decided to construct pATH which expresses, under the T7-regulated promoter, a cytoplasmic form of AT (Ath) with a C-terminal extension of six histidine residues (Figure 1). Ath was purified from BL21-(DE3) pATH-induced cells and was found to be devoid of any contamination with TolB from Coomassie blue-stained SDS-PAGE analyses (Figure 2). The N-terminal sequence of purified Ath was found to lack the N-terminal methionine residue as predicted from its mass spectrum.

In agreement with what was previously observed with the N-terminal domain of colicin N (42), the far-UV circular dichroism (CD) spectrum of Ath shows no significant amount of ordered secondary structure (Figure 4) and was similar to that of AT1 (27). The HSQC spectra of ^{15}N -labeled Ath result in a significant amount of poorly dispersed signals superimposing in the middle of the spectra (Figure 5), confirming this lack of structure, which is in agreement with the CD data.

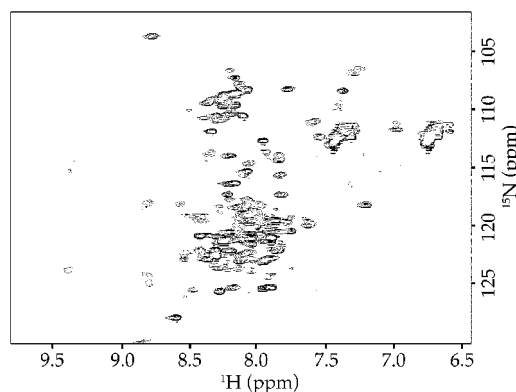


FIGURE 5: 2D $^1\text{H}-^{15}\text{N}$ HSQC spectrum of Ath. NMR analyses of 0.3 mM ^{15}N -labeled Ath in 50 mM NaF and 50 mM KPO_4 (pH 6.8), recorded on a Varian Inova 800 MHz spectrometer at 300 K.

Formation of the Complex of TolAIII with Ath. The binding of Ath to TolAIII derivatives was checked using several biochemical methods. Purified TolAIII2 and TolAIII3 were analyzed by a Western blot and dot blot, which were incubated with 200 nM Ath followed by immunodetection with 1C11 monoclonal antibody (mAb) directed against the colicin domain. Under these conditions, the Ath protein was found to recognize TolAIII2 and TolAIII3. Similar results were previously obtained with AT1 (the same protein as Ath but without the hexahistidine tag) and TolAIII1 (30).

To confirm this result and to analyze the effect of the ionic strength on the interaction, coprecipitation experiments were carried out using TolAIII2 or TolAIII3 immobilized on a metal affinity support which was further incubated with AT1 protein (Ath containing a hexahistidine tag was not used). Besides faint amounts of AT1 unspecifically recovered in the eluted fractions in absence of TolA derivatives (since no histidine tag is present in AT1), we observed large amounts of AT1 copurifying with TolAIII2 and TolAIII3 whatever the ionic strength (between 0 and 500 mM NaCl) (Figure 2). This result indicated that the interaction between

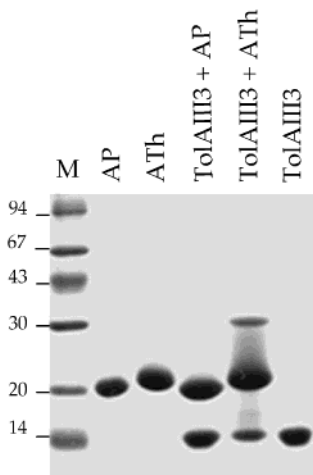


FIGURE 6: Results of SDS-PAGE shift experiments with the ATh-TolAIII3 complex. Protein samples (AP, for the colicin A pore-forming domain, 5 μg ; ATh, 6 μg ; TolAIII3, 3 μg ; and the mixture of TolAIII3 with the two domains of colicin A) were incubated for 20 min at room temperature in a final volume of 15 μL and further analyzed by SDS-PAGE stained with Coomassie blue. Size markers (M) are indicated in kilodaltons.

the C-terminal domain of TolA and the N-terminal domain of colicin A did not occur via electrostatic interactions.

Immunoprecipitation experiments using mAb IC11, which recognizes an epitope located within the N-terminal sequence of ATh, were also checked with ATh and TolAIII derivative mixtures. Coomassie blue-stained SDS-PAGE analyses indicated that TolAIII2 and TolAIII3 co-immunoprecipitate with ATh (data not shown). SDS-PAGE shift experiments (30) were performed with the purified ATh and TolAIII3. A TolAIII3-ATh protein complex could be clearly detected having a relative electrophoretic mobility corresponding to a heterodimer, while this complex slightly dissociated into monomeric forms upon migration (Figure 6). However, no complex was detected if protein samples were incubated in 0.1% SDS prior to loading (not shown) or if a protein control, the pore-forming domain of colicin A (AP) instead of ATh, was added with TolAIII3.

Gel filtration experiments using ATh, TolAIII3, and TolAIII3 with ATh, loaded at the same concentration and in the same buffer used for NMR interaction analyses, further indicated the formation of a heterodimer.

Structural Characterization of the Interaction between ^{15}N -Labeled TolAIII Derivatives and ATh. The interaction between ATh and TolAIII3 is expected to induce changes in the magnetic environment and in the dynamics of the nuclei at the interface of the two molecules giving rise to chemical shift and line width variations of the corresponding signals. The HSQC spectrum of ^{15}N -labeled TolAIII3 is significantly altered after addition of unlabeled ATh (Figure 7A). Chemical exchange between the free and complexed forms of TolAIII3 is slow on a millisecond time scale as resonances of free TolAIII3 progressively vanish and the complexed TolAIII3 resonances appear while ATh is added step by step. Backbone amide ^1H resonances observed for complexed TolAIII3 appear to be less dispersed than those of free TolAIII3, and most peaks appear to be severely broadened. A significant number of resonances may not even be visible. The integrity of the interacting proteins was verified after the NMR titration by SDS-PAGE analysis and

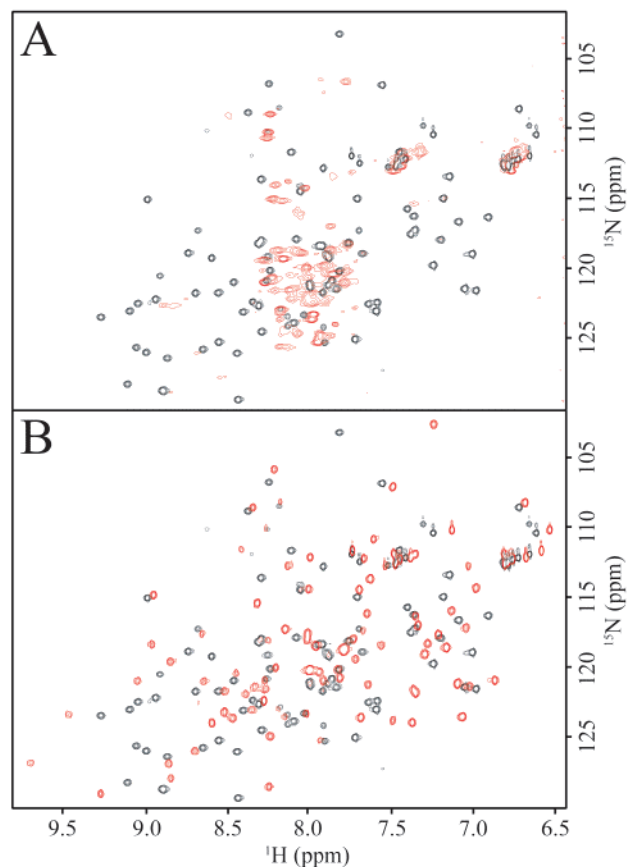


FIGURE 7: 2D ^1H - ^{15}N HSQC spectra of TolAIII3, the TolAIII3-ATh complex, and the TolAIII3-g3p N1 complex. (A) NMR studies of ^{15}N -labeled TolAIII3 interacting with ATh. 2D ^1H - ^{15}N HSQC spectra of 0.1 mM ^{15}N -labeled TolAIII3 in the absence (black) or in the presence of an excess (red) of unlabeled ATh, recorded on a Varian Inova 800 MHz spectrometer at 300 K. (B) NMR studies of ^{15}N -labeled TolAIII3 interacting with g3p N1. 2D ^1H - ^{15}N HSQC spectra of 0.1 mM ^{15}N -labeled TolAIII3 in the absence (black) or in the presence of an excess (red) of unlabeled g3p N1, recorded under the same conditions described for panel A.

was found to be identical to that of purified protein stocks, without any degradation. To ensure there was no formation of protein aggregates in the NMR tube, the diffusion constant of TolAIII3 was measured before ($1.3 \times 10^{-6} \text{ cm}^2/\text{s}$) and after ($0.5 \times 10^{-6} \text{ cm}^2/\text{s}$) addition of ATh using a DOSY NMR experiment (43). As the diffusion coefficient of a protein is inversely proportional to the effective hydrodynamic radius of that protein (44), the observed ratio of 2.6 is compatible with the formation of a TolAIII3-ATh heterodimer. The advantage of estimating a diffusion coefficient by DOSY NMR, compared to other techniques (such as gel filtration), is that the observed system is exactly the same as for the rest of the NMR study. In particular, the protein concentration is unchanged (among other conditions), which thus avoid possible artifacts due to variations in the oligomerization state of the complex.

Similar spectral characteristics of the TolAIII3-ATh complex are observed for proteins with no well-defined tertiary contacts. In such proteins lacking native tertiary structure, conformational fluctuations on a microsecond to millisecond time scale yield severe resonance broadening. Also, interactions responsible for ^1H chemical shift dispersion (such as dipolar interactions or ring current effects) are averaged out by conformational fluctuations (45).

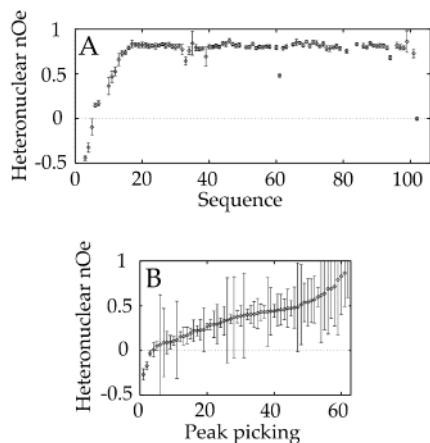


FIGURE 8: Backbone $\{^1\text{H}\}-^{15}\text{N}$ steady-state heteronuclear nOe values for free TolAIII3 and TolAIII3 complexed with unlabeled ATh. (A) Sequence assignment of backbone $\{^1\text{H}\}-^{15}\text{N}$ steady-state heteronuclear nOe values for free TolAIII3. (B) Backbone $\{^1\text{H}\}-^{15}\text{N}$ steady-state heteronuclear nOe values for TolAIII3 when complexed with (unlabeled) ATh. Values are arbitrarily ranked in increasing order.

Additional experiments were carried out to characterize the ATh-complexed form of TolAIII3. The propensity to form secondary structure elements can usually be assessed by far-UV circular dichroism (CD). Comparison of the CD spectrum of the TolAIII3–ATh complex (Figure 4) with the theoretical CD spectrum of a noninteracting equimolar mixture of TolAIII3 and ATh suggests that the secondary structure elements are mostly preserved in the complex, probably resulting from the remaining ordered secondary structure of TolAIII3. The apparent discrepancy with the poorly resolved NMR spectra can be easily resolved by noting that CD spectroscopy only monitors the backbone conformation while the chemical shift is affected by both short-range and long-range electronic effects. In the CD experiments, however, both partners can contribute to the signal and the spectra have to be interpreted very carefully. The same obstacle is also encountered with other techniques such as ANS fluorescence which is used to characterize the global hydrophobic exposure. Near-UV CD of the complex did not give information about TolAIII3 tertiary structure due to the low extinction coefficient of TolAIII3 compared to that of ATh. TolAIII3 itself contains no tryptophan residues to enable tryptophan fluorescence observation.

To characterize the local dynamics of TolAIII3, motion of the backbone amide NH bonds was investigated on the picosecond to nanosecond time scale by measuring the steady-state $\{^1\text{H}\}-^{15}\text{N}$ heteronuclear nuclear Overhauser effect (46) on ^{15}N -labeled samples (Figure 8). Extensive peak picking of backbone NH resonances was carried out in the spectra of both free and complexed TolAIII3. Free TolAIII3 $\{^1\text{H}\}-^{15}\text{N}$ nOe values could be assigned. They are mainly around 0.8, indicating motional restriction of the backbone, as expected of a well-folded protein (47). Lower values could be assigned to the beginning of the chain and to residue Gly 61. Complexed TolAIII3 $\{^1\text{H}\}-^{15}\text{N}$ nOe values could not be assigned, and some of them may actually be averaged on several residues due to severe overlaps in the spectrum. Nonetheless, valuable information can be derived for a global analysis of these data. Complexed TolAIII3 displays significantly lower $\{^1\text{H}\}-^{15}\text{N}$ nOe values. These lower positive values indicate partially restricted motion of the backbone,

as described for proteins in the molten globule state (48). This demonstrates that complexed TolAIII3 is less structured than the free protein. However, it is not unstructured as mostly negative values would have been expected for random coil conformations. Negative $\{^1\text{H}\}-^{15}\text{N}$ nOe values can be observed either for small molecules which tumble rapidly or for completely disordered proteins (described as random coils) where fast segmental motions dominate (49). The observation of positive nOe values for complexed TolAIII3 clearly demonstrates that secondary structure elements are mostly preserved, even if lower values (as compared to that of the free protein) support additional flexibility.

Additional binding assays were performed via HSQC spectroscopy. The same type of effect of ATh on TolAIII3 (peak broadening and poor dispersion) could be observed on reduced ^{15}N -labeled TolAIII2 as well as on the longer ^{15}N -labeled TolAIII1 construct. The same type of effect could also be observed with the entire colicin A instead of the ATh domain only. The specificity of TolAIII conformational changes was asserted by a control spectrum of a protein unrelated to the system presented here, the ^{15}N -labeled ribosome recycling factor (RRF), in the presence of ATh and by a second control of ^{15}N -labeled TolAIII3 with trypsin-digested ATh at the same concentration as the entire ATh. In both cases, ATh does not modify the RRF HSQC spectrum and digested ATh does not modify the TolAIII3 HSQC spectrum.

In the previous structural data reported for the g3p N1–TolAIII complex, no structural changes in TolAIII structure have been observed. Any structural changes between free and bound TolAIII could not be detected with complexed TolAIII (29) in the absence of a free TolAIII crystal structure. While in NMR experiments (24) only ^{15}N -labeled g3p N1 was observed, nothing about TolAIII structural changes could be deduced. For this reason, we have investigated using a similar approach the effect of g3p N1 binding on TolAIII conformation.

NMR Characterization of the Interaction between g3p N1 and ^{15}N -Labeled TolAIII3. From the crystal structure of a fusion protein containing g3p N1 and TolAIII (29), TolAIII3 has been found to adopt a definite structure. However, the effect of g3p N1 binding on the conformation of TolAIII3 cannot be seen in the absence of high-resolution structural data for free TolAIII3. We investigated the effect of g3p N1 binding on TolAIII3 directly by heteronuclear NMR using the same approach described for the ATh–TolAIII3 complex.

Plasmid pP31 encoding g3p N1 of M13 phage was constructed. It expressed the natural signal sequence of g3p followed by its first 71 residues and a C-terminal tag of six histidine residues (Figure 1). The protein was purified from the periplasm by an osmotic shock procedure. Like that of TolAIII3, expression of g3p N1 in the periplasm induces the release of periplasmic proteins (50), and a fraction of g3p N1 was purified from the culture supernatant. SDS–PAGE and MALDI–TOF analyses of purified g3p N1, in the absence of a reducing agent, indicated that the protein is monomeric (Figure 2), having the expected mass spectrum.

A titration of the formation of the complex of g3p N1 and ^{15}N -labeled TolAIII3 was monitored by heteronuclear $^1\text{H}-^{15}\text{N}$ HSQC spectroscopy (Figure 7B). Most TolAIII3 $^1\text{H}-^{15}\text{N}$ correlation peaks shift. This confirms the binding

of g3p N1, but it also indicates that the binding affects more than the protein–protein interface, possibly inducing conformation changes in TolAIII3. Chemical exchange between the free and complexed forms of TolAIII3 is slow on a millisecond time scale, as there is no coalescence or signal averaging between the two forms during the titration. Therefore, it is not possible to infer the resonance assignments of the complexed form from the resonance assignments of the free form of TolAIII3 directly from the titration. The dispersion of the bound form of TolAIII3 backbone amide ^1H resonances is good enough to confirm that this form has a definite tertiary structure.

DISCUSSION

The TolA protein plays a central role in the import process of filamentous bacteriophage DNA and group A colicins. The C-terminal domain of TolA (TolAIII) has been shown to interact with g3p and colicins (24, 30). Two distinct regions within TolAIII have been found to be necessary for the interactions with colicins A and E1 (28) (Figure 1), and residues participating in the contact of TolAIII with g3p have been determined to be mostly located in the first α -helix and the last β -strand of TolAIII (29). Residues within the translocation domain of colicins A and N that are important for TolAIII interaction have also been characterized (51, 52). The constants of dissociation of the N-terminal domains of colicins A and E1 from the C-terminal domain of TolA (TolAIII) were found to be in the micromolar range (30), while similar K_D values were determined for the binding of TolA to the N-terminal domain of colicin N (42). However, it is still unknown how the interaction of the C-terminal domain of TolA with the N-terminal domain of colicins triggers the entry of the colicin lethal domain and if the same molecular mechanism is used for phage genome entry.

To study the TolA–colicin A interaction by NMR, we have constructed and purified shortened C-terminal domains of TolA (TolAIII2 and TolAIII3 containing 97 and 93 residues, respectively). By comparison with these new constructs, TolAIII1 (132 residues) was shown to contain a mobile region corresponding to its N-terminal sequence. As a result of structural disorder, this same region could not be observed in the crystal structure of a g3p N1–TolAIII fusion protein (29). The NMR-derived topology of secondary structure elements of TolAIII3 was found to consist of three α -helices and three β -strands, was identical in TolAIII2 (not shown), and is not significantly different from the topology observed in the g3p N1–TolAIII crystal structure. However, our NMR data show that TolAIII3 could undergo significant conformational changes upon binding with g3p N1. Therefore, the determination of the tertiary structure of free TolAIII3 is essential for interpretation of the ongoing studies of this protein. The determination of the high-resolution three-dimensional (3D) solution structure of free TolAIII3 is currently in progress and will allow a better comparison with the crystal structure of complexed TolAIII.

NMR (HSQC) spectra of g3p N1 binding to ^{15}N -labeled TolAIII3 lead to a well-structured complex, while in contrast, binding of the N-terminal domain of colicin A results in a flexible conformation with the C-terminal domain of TolA in either the presence or absence of its disulfide bridge. This conformation is characterized by a certain structural pro-

pensity (observed by circular dichroism) but lacks a rigid tertiary structure (as derived from NMR peak widths and dispersion as well as heteronuclear NOEs). Increased protein flexibility upon ligand binding is rather unusual. Such an effect, though small in amplitude, has already been observed in several cases involving small compounds, nucleic acids, and peptides (53). Our study provides an interesting experimental system for reassessing the conventional view that binding leads to restricted conformational flexibility (54). However, the effects of conformational fluctuations on NMR spectra (peak broadening and poor shift dispersion) make NMR investigations of poorly folded proteins difficult. Assigning the resonance of the AT-hetero-complexed form of TolAIII3 is challenging but necessary before the invaluable information necessary to characterize structure and dynamics at atomic resolution can be exploited.

Here we show that in vitro the translocation domain of colicin A has a strongly perturbing effect on the tertiary structure of TolAIII, and thus presumably also on the whole Tol–Pal system within the periplasm of *E. coli*. In vivo and in vitro, the same TolAIII3 domain has previously been found to interact with the Pal lipoprotein. Similarly, TolA interacts with Pal in vivo, but no interaction was detected with TolA deleted of its C-terminal domain (6). This interaction which allows the inner membrane-anchored TolA to link the outer membrane-anchored Pal lipoprotein has been suggested to have outer membrane-stabilizing effects (6). As the Tol–Pal system plays a critical role in maintaining the integrity of the outer membrane, one could imagine that the translocation strategy of group A colicins consists of breaking the TolA–Pal link between the two membranes, thus fragilizing the bacterial envelope and allowing the lethal domain of the colicin to translocate through the outer membrane more freely. This is not sufficient however as (by definition) fragilized *tol–pal* mutants exhibit a tolerant phenotype so that colicin translocation is inhibited. The import of colicin may depend on both a functional Tol–Pal system triggering colicin translocation and a destabilized cell envelope. The analyses of the TolA–Pal interaction (6) during colicin import will be investigated to observe if this interaction is preserved or abolished. Similarly, the periplasmic production of colicin translocation domains (41) and of the g3p N1 domain would be useful tools for analyzing the effect of the overproduction of periplasmic domains on the TolA–Pal interaction.

The role of the different Tol proteins involved in the colicin import process is still unknown, but the different locations of the TolA, TolB, and TolR binding regions within the N-terminal domain of colicin A might indicate that sequential interactions occur during the translocation of the N-terminal domain of group A colicins (52). However, a minimal requirement of the Tol–Pal system is found with colicin E1 and N which required only the TolA and TolQ proteins (15, 51).

It has previously been proposed that the pH-induced transition of the colicin A C-terminal domain from the folded structure to a molten globule may facilitate its transmembrane insertion (55). It remains to be determined if the flexibility of TolAIII, which is induced upon binding the colicin AT-hetero domain at neutral pH, corresponds to a molten globular state which could contribute to the translocation of colicin by disrupting at least the TolA–Pal interaction.

TolAIII3 behaves differently when bound to g3p N1 or to ATh. The two interacting partners exhibit different electrostatic behavior and 3D structures; whereas the N-terminal domain of g3p (theoretical pI of 5.3) is a highly stable domain formed by a six-stranded β -barrel (56), the N-terminal domain of colicin A (theoretical pI of 9.0) is poorly structured. We have also shown from binding assays with increasing ionic strength that the interaction between the C-terminal domain of TolA and the N-terminal domain of colicin A is not electrostatically driven. As derived from the crystal structure, the binding between TolAIII and g3p N1 occurs via both hydrophobic and electrostatic interactions (29) (residues in interaction are shown in Figure 1). Is the translocation strategy for the genome of filamentous phages similar to that of the lethal domain of group A colicins? We have shown that g3p N1 has a less drastic effect than the N-terminal domain of colicin A on the 3D structure of TolAIII. The repercussions of this interaction on the whole Tol–Pal system have to be determined to better understand the translocation process. However, these observations might reflect the fact that after the import process, colicins directly kill the cells while after DNA import, Ff bacteriophages need the machinery of functional cells to multiply. Moreover, when Ff phages are assembled and secreted, cells have been shown to remain fully viable (57). A better knowledge of the organization and physiological role of the Tol–Pal system and an investigation of all the different interactions, even transient, that might take place between the colicins or g3p and the Tol–Pal proteins is necessary to understand the mechanism of import of Ff phage DNA and colicins across the cell envelope.

The interaction of TolAIII with its TolB and Pal partners is now under investigation using ^{15}N -labeled TolAIII3. Preliminary experiments have indicated that the interaction of TolB on TolAIII1 modifies the resonances of some residues without affecting the flexibility of TolAIII1. These experiments together with binding affinity constant measurements and interaction experiments involving different partners will help us to understand the multiple interactions of the Tol–Pal proteins and the effects of colicins and of the g3p minor coat protein on the Tol–Pal system.

ACKNOWLEDGMENT

We thank Olivier Bornet for data from preliminary NMR experiments, Gareth Morris for the DOSY software, Cécile Abdou for constructing plasmid pP3I, Norbert Rolland for providing the RRF sample, Jacques Bonicel for determining the N-terminal amino acid sequences and performing mass spectrometry experiments together with Michel Jacquinet, and James Sturgis for fruitful discussions and careful reading of the manuscript.

REFERENCES

- Derouiche, R., Bénédicti, H., Lazzaroni, J.-C., Lazdunski, C., and Llobès, R. (1995) *J. Biol. Chem.* 270, 11078–11084.
- Lazzaroni, J. C., Vianney, A., Popot, J.-L., Bénédicti, H., Samatey, F., Lazdunski, C., Portalier, R., and Geli, V. (1995) *J. Mol. Biol.* 246, 1–7.
- Germon, P., Clavel, T., Vianney, A., Portalier, R., and Lazzaroni, J. C. (1998) *J. Bacteriol.* 180, 6433–6439.
- Bouveret, E., Derouiche, R., Rigal, A., Llobès, R., Lazdunski, C., and Bénédicti, H. (1995) *J. Biol. Chem.* 270, 11071–11077.
- Ray, M. C., Germon, P., Vianney, A., Portalier, R., and Lazzaroni, J. C. (2000) *J. Bacteriol.* 182, 821–824.
- Cascales, E., Gavioli, M., Sturgis, J. N., and Llobès, R. (2000) *Mol. Microbiol.* 38, 904–915.
- Lazzaroni, J.-C., and Portalier, R. (1992) *Mol. Microbiol.* 6, 735–742.
- Clavel, T., Germon, P., Vianney, A., Portalier, R., and Lazzaroni, J. C. (1998) *Mol. Microbiol.* 29, 359–367.
- Webster, R. (1991) *Mol. Microbiol.* 5, 1005–1011.
- Bernadac, A., Gavioli, M., Lazzaroni, J. C., Raina, S., and Llobès, R. (1998) *J. Bacteriol.* 180, 4872–4878.
- Llobès, R., Cascales, E., Walburger, A., Bouveret, E., Lazdunski, C., Bernadac, A., and Journet, L. (2001) *Res. Microbiol.* 152, 523–529.
- Derouiche, R., Gavioli, M., Bénédicti, H., Prilipov, A., Lazdunski, C., and Llobès, R. (1996) *EMBO J.* 15, 6408–6415.
- Rigal, A., Bouveret, E., Llobès, R., Lazdunski, C., and Bénédicti, H. (1997) *J. Bacteriol.* 179, 7274–7279.
- Gaspar, J., Thomas, J., Marolda, C., and Valvano, M. (2000) *Mol. Microbiol.* 38, 262–275.
- Lazdunski, C. J., Bouveret, E., Rigal, A., Journet, L., Llobès, R., and Bénédicti, H. (1998) *J. Bacteriol.* 180, 4993–5002.
- Elkins, P., Bunker, A., Cramer, W. A., and Stauffacher, C. (1997) *Structure* 5, 443–458.
- Parker, M., Postma, J. P., Pattus, F., Tucker, A., and Tsenoglou, D. (1992) *J. Mol. Biol.* 224, 639–657.
- Vetter, I., Parker, M., Tucker, A., Lakey, J., Pattus, F., and Tsenoglou, D. (1998) *Structure* 6, 863–873.
- Wiener, M., Freymann, D., Ghosh, P., and Stroud, R. M. (1997) *Nature* 385, 461–464.
- Guihard, G., Boulanger, P., Bénédicti, H., Llobès, R., Besnard, M., and Letellier, L. (1994) *J. Biol. Chem.* 269, 5874–5880.
- Duché, D., Letellier, L., Geli, V., Bénédicti, H., and Baty, D. (1995) *J. Bacteriol.* 177, 4935–4939.
- Lubkowski, J., Hennecke, F., Plückthun, A., and Wlodawer, A. (1998) *Nat. Struct. Biol.* 5, 140–147.
- Holliger, P., Riechmann, L., and Williams, R. L. (1999) *J. Mol. Biol.* 288, 649–657.
- Riechmann, L., and Holliger, P. (1997) *Cell* 90, 351–360.
- Click, E., and Webster, R. (1998) *J. Bacteriol.* 180, 1723–1728.
- Levengood, S., Beyer, W., Jr., and Webster, R. (1991) *Proc. Natl. Acad. Sci. U.S.A.* 88, 5939–5943.
- Derouiche, R., Llobès, R., Sasso, S., Bouteille, H., Oughideni, R., Lazdunski, C., and Loret, E. (1999) *Biospectroscopy* 5, 189–198.
- Bénédicti, H., Lazdunski, C., and Llobès, R. (1991) *EMBO J.* 10, 1989–1991.
- Lubkowski, J., Hennecke, F., Plückthun, A., and Wlodawer, A. (1999) *Structure* 7, 711–722.
- Derouiche, R., Zeder-Lutz, G., Bénédicti, H., Gavioli, M., Rigal, A., Lazdunski, C., and Llobès, R. (1997) *Microbiology* 143, 3185–3192.
- Ansaldi, M., Lepelletier, M., and Mejean, V. (1996) *Anal. Biochem.* 234, 110–111.
- Ghrayeb, J., Kimura, H., Takahara, M., Hsiung, H., Masui, Y., and Inouye, M. (1984) *EMBO J.* 3, 2437–2442.
- Llobès, R., Baty, D., and Lazdunski, C. (1986) *Nucleic Acids Res.* 14, 2621–2636.
- Tabor, S., and Richardson, C. (1985) *Proc. Natl. Acad. Sci. U.S.A.* 82, 1074–1078.
- Wishart, D. S., Bigam, C. G., Yao, J., Abildgaard, F., Dyson, H. J., Oldfield, E., Markley, J. L., and Sykes, B. D. (1995) *J. Biomol. NMR* 6, 135–140.
- Levengood-Freyermuth, S., Click, E., and Webster, R. (1993) *J. Bacteriol.* 175, 222–228.
- Wan, E. W., and Baneyx, F. (1998) *Protein Expression Purif.* 14, 13–22.
- Deprez, C., Blanchard, L., Simorre, J.-P., Gavioli, M., Guerlesquin, F., Lazdunski, C., Llobès, R., and Marion, D. (2000) *J. Biomol. NMR* 18, 179–180.

39. Wishart, D. S., and Sykes, B. D. (1994) *J. Biomol. NMR* 4, 171–180.
40. Knibiehler, M., Howard, S. P., Baty, D., Géli, V., Llobès, R., and Lazdunski, C. (1989) *Eur. J. Biochem.* 181, 109–113.
41. Bouveret, E., Rigal, A., Lazdunski, C., and Bénédicti, H. (1998) *Mol. Microbiol.* 27, 143–157.
42. Raggett, E., Bainbridge, G., Evans, L., Cooper, A., and Lakey, J. (1998) *Mol. Microbiol.* 28, 1335–1343.
43. Johnson, C. S., Jr. (1999) *Prog. Nucl. Magn. Reson. Spectrosc.* 34, 203–256.
44. Jones, J. A., Wilkins, D. K., Smith, L. J., and Dobson, C. M. (1997) *J. Biomol. NMR* 10, 199–203.
45. Dyson, H., and Wright, P. (1998) *Nat. Struct. Biol.* 5, 499–503.
46. Kay, L. E., Torchia, D. A., and Bax, A. (1989) *Biochemistry* 28, 8972–8979.
47. Tsan, P., Hus, J.-C., Caffrey, M., Marion, D., and Blackledge, M. (2000) *J. Am. Chem. Soc.* 122 (23), 5603–5612.
48. Eliezer, D., Yao, J., Dyson, H. J., and Wright, P. E. (1998) *Nat. Struct. Biol.* 5, 148–155.
49. Nagadoi, A., Nakazawa, K., Uda, H., Okuno, K., Maekawa, T., Ishii, S., and Nishimura, Y. (1999) *J. Mol. Biol.* 287, 593–607.
50. Rampf, B., Bross, P., Vocke, T., and Rashed, I. (1991) *FEBS Lett.* 280, 27–31.
51. Gokce, I., Raggett, E., Hong, Q., Virden, R., Cooper, A., and Lakey, J. (2000) *J. Mol. Biol.* 304, 621–632.
52. Journet, L., Bouveret, E., Rigal, A., Llobès, R., Lazdunski, C., and Bénédicti, H. (2001) *Mol. Microbiol.* 42, 331–344.
53. Stone, M. J. (2001) *Acc. Chem. Res.* 34, 379–388.
54. Forman-Kay, J. D. (1999) *Nat. Struct. Biol.* 6, 1086–1087.
55. van der Goot, F., Gonzalez-Manas, J., Lakey, J., and Pattus, F. (1991) *Nature* 354, 408–410.
56. Holliger, P., and Riechmann, L. (1997) *Structure* 5, 265–275.
57. Russel, M., Linderth, N., and Sali, A. (1997) *Gene* 192, 23–32.

BI0157262